Hindawi Publishing Corporation
International Journal of Antennas and Propagation
Volume 2016, Article ID 5429510, 9 pages
http://dx.doi.org/10.1155/2016/5429510

Research Article

Nantenna for Standard 1550 nm Optical Communication Systems

Waleed Tariq Sethi,[1,2] Hamsakutty Vettikalladi,[3] Habib Fathallah,[1,3] and Mohamed Himdi[2]

[1] *KACST Technology Innovation Center in Radio Frequency and Photonics for the e-Society (RFTONICS), King Saud University, Riyadh 11451, Saudi Arabia*
[2] *Institute of Electronics and Telecommunications of Rennes University (IETR), University of Rennes 1, 35700 Rennes, France*
[3] *Electrical Engineering Department, King Saud University, P.O. Box 800, Riyadh 11421, Saudi Arabia*

Correspondence should be addressed to Waleed Tariq Sethi; wsethi@ksu.edu.sa

Received 26 February 2016; Accepted 3 July 2016

Academic Editor: Jaume Anguera

Nanoscale transmission and reception technologies will play a vital role and be part of the next generation communication networks. This applies for all application fields including imaging, health, biosensing, civilian, and military communications. The detection of light frequency using nanooptical antennas may possibly become a good competitor to the semiconductor based photodetector because of the simplicity of integration, cost, and inherent capability to detect the phase and amplitude instead of power only. In this paper, authors propose simulated design of a hexagonal dielectric loaded nantenna (HDLN) and explore its potential benefits at the standard optical C-band (1550 nm). The proposed nantenna consists of "Ag-SiO_2-Ag" structure, consisting of "Si" hexagonal dielectric with equal lengths fed by "Ag" nanostrip transmission line. The simulated nantenna achieves an impedance bandwidth of 3.7% (190.9 THz–198.1 THz) and a directivity of 8.6 dBi, at a center frequency of 193.5 THz, covering most of the ITU-T standard optical transmission window (C-band). The hexagonal dielectric nantenna produces $HE_{20\delta}$ modes and the wave propagation is found to be end-fire. The efficiency of the nantenna is proven via numerical expressions, thus making the proposed design viable for nanonetwork communications.

1. Introduction

The recent developments in nanotechnology have motivated the researchers to explore and design optical (nano)antennas by downscaling the radio frequency (RF) antennas towards optical frequencies. Thus, the familiar design principles and operational concepts of RF and microwave antenna technology can be directly applied to the rapidly emerging area of optical antennas [1–3]. The reduction in the size of electronic and optoelectronic components and their integration into nanosystems, by the use of nanotechnology, is the basis of a nanonetwork. The communication between the integrated components would achieve a complex task, in distributed manner, enabling unique applications of nanotechnology [4]. The operation can be performed via optical antennas called nantennas. Besides capturing/enhancing optical light, nantennas find their usefulness in applications like optoelectronic devices, optical transmitters and receivers, solar cells, nanonetworks, sensing applications, artificial spectroscopy, and nanophotonics circuit integration [5, 6]. At present, limited literature is available on nantenna designs that include configurations such as dipoles, bow ties, Yagi-Uda, split ring, and spiral nantennas [7–13]. Apart from these, many of the other state-of-the-art nantenna designs [14–17] are mostly based on extensive theoretical and numerical analysis aided by electromagnetic simulators due to limited availability and very expensive cost of the nanofabrication facilities. Even after fabrication, the characterization and measurement at present are an unrealistic task to achieve. The communication between devices in the nanonetworks is still an unsolved challenge. The miniaturization of classical antennas with

usage of nanomaterials is one solution, proposed by the authors, as one of the main objectives of this paper.

In traditional RF domain, metals that behave as perfect electric conductor are used to make majority of antennas. These conductors designed at microwave and millimeter wave frequencies are encountered with losses, although there are subsequent techniques available to subside these losses [3]. Alternatively, a technique exists to avoid these conduction losses by making use of antennas having dielectric materials. Dielectric resonators (DR), proposed in 1939 [18], are nonmetallized dielectric objects that function similarly to metallic cavities. With the low loss dielectric material, the dielectric resonator antenna (DRA) has some advantages over the metallic ones such as high radiation efficiency due to lack of surface waves, small size proportional to wavelength (λ_0), wide impedance bandwidth, many feeding arrangements, and different excitation methods with several modes producing broadside or end-fire radiation patterns [19–24].

In general, DRAs exhibit infinite resonant mode when excited in an ideally isolated environment. With appropriate selection of excitation modes, the DRAs can be used as an efficient radiator or a loader with appropriate end-fire or broadside radiation patterns. Antenna behavior and far field radiation patterns could be predicted with the known and available knowledge of DR's resonant modes [22]. DRAs are normally made of ceramics with high permittivity, that is, $\varepsilon_r = (10–100)$ for acquiring wide bandwidth, and commonly placed on a finite ground plane with a substrate of similar dimensions. The feeding of DRAs can be done via a coaxial or microstrip line feed [20]. Numerous geometries of DRAs are available which include cylindrical, rectangular, half-cylindrical, spherical, triangular, and hexagonal shapes [25–30]. The cylindrical DR is mostly used offering one of the three resonating modes, $TE_{01\delta}$, $TM_{01\delta}$, and $HE_{11\delta}$, from many available modes, in applications involving radiations behaving like a short vertical electric and magnetic dipole and as a horizontal magnetic dipole [22]. Here, vertical and horizontal refer to the directions that are parallel and orthogonal, respectively, to the cylindrical axis.

In this paper, in order to benefit from the wide band characteristics and efficient radiation properties of DR as a loading element, we propose and explore the design of a hexagonal dielectric loaded nantenna (HDLN). The design is inspired from the reference antenna at low radio frequencies [25]. The proposed nantenna consists of a multilayer structure having "SiO_2" sandwiched between two silver "Ag" sheets. The radiating element is an equal sided hexagonal shaped "Si" dielectric loaded material. The whole nantenna structure is excited via a nanostrip transmission line made from a noble silver metal "Ag" whose conductive properties are calculated via the Drude model [31]. The antenna achieves an impedance bandwidth of 3.7% (190.9 THz–198.1 THz) with a directivity of 8.6 dBi at the frequency of interest. The obtained results make the proposed nantenna a possible solution for future nanophotonics and nanoscale communication devices.

2. Proposed Nantenna Design

In the present investigation, the optical HDLN is designed for operating at a center frequency of 193.5 THz, which corresponds to an operating wavelength of 1.55 μm. The proposed geometrical configuration (side view and top view with field vectors) of the HDLN is shown in Figures 1(a) and 1(b). The design consists of "SiO_2" substrate with a thickness of $h_1 = 0.150\,\mu$m, $\varepsilon_r = 2.1$, and loss tangent $\tan\delta = 0.003$ at $f = 100$ THz [32] sandwiched between two silver metal layers. The partial ground plane is on the bottom side of "SiO_2" substrate with thickness of $t = 0.010\,\mu$m and dimensions $L_g \times W_g = 1.95 \times 2\,\mu$m, while on the top side a nanostrip transmission line with thickness $h_2 = 0.025\,\mu$m is located. The substrate dimensions are taken as $W_s \times L_s = 5 \times 5\,\mu\text{m}^2$. The hexagonal dielectric is made of "Si" with $\varepsilon_r = 11.9$ and estimated loss tangent, $\tan\delta = 0.0025$ [32] at $f = 100$ THz, is excited via the 50 Ω silver nanostrip feedline that has dimensions of $W_f = 0.067\,\mu$m and $L_f = 0.186\,\mu$m. A small substrate with thickness $h_3 = 0.015\,\mu$m made from "SiO_2" has been introduced between the hexagon and the nanostrip to widen the achieved bandwidth. The dimensions of hexagonal dielectric are calculated from (1) [3] by inscribing the hexagon inside a circle and equating the areas of both designs, thus giving optimized equal side lengths of hexagon as $s = 1\,\mu$m and thickness ($\lambda_g/4 < h < \lambda_g/2$) $h = 0.377\,\mu$m:

$$\pi a_e^2 = \frac{3\sqrt{3}}{2} s^2, \tag{1}$$

where a_e is area of the circle and s is side of the hexagon. Since at optical frequencies metals appear with a negative permittivity, complex permittivity "ε_{Ag}" of silver (Ag) was calculated from (2) explained by the Drude model [31]:

$$\varepsilon_{Ag} = \varepsilon_0 \left\{ \varepsilon_\alpha - \frac{f_p^2}{[f\,(f + i\gamma)]} \right\} = -128 + j3.28, \tag{2}$$

where $\varepsilon_0 = 8.85 \times 10^{-12}$ [F/m], $\varepsilon_\alpha = 5$, plasmonic frequency $f_p = 2175$ THz, f is central frequency, and collision frequency $\gamma = 4.35$ THz. The proposed model has taken into account the conductive and dielectric losses and has been simulated using commercially available EM simulator CST Microwave Studio 2012 [33] based on FIT numerical technique. Figure 1(b) illustrates the antenna operating in the transmitting (Tx) mode by means of propagation vector orientation (k). The magnetic and electric field distributions of the hexagonal dielectric and nanostrip waveguide, along with the wave propagation in the y-axis, are also shown. Optical nantennas can be excited with a few known techniques being (1) coupling of light using the so-called nanotapers [34, 35]. Since nanoantennas cannot handle much power because of their small footprints, this makes them ideal candidates for being excited by microlasers such as microdisks and photonic crystal lasers. Another method of excitation that outperforms the former microlaser based technique by reducing the reflection induced power loss exploits (2) slot dielectric waveguides [36].

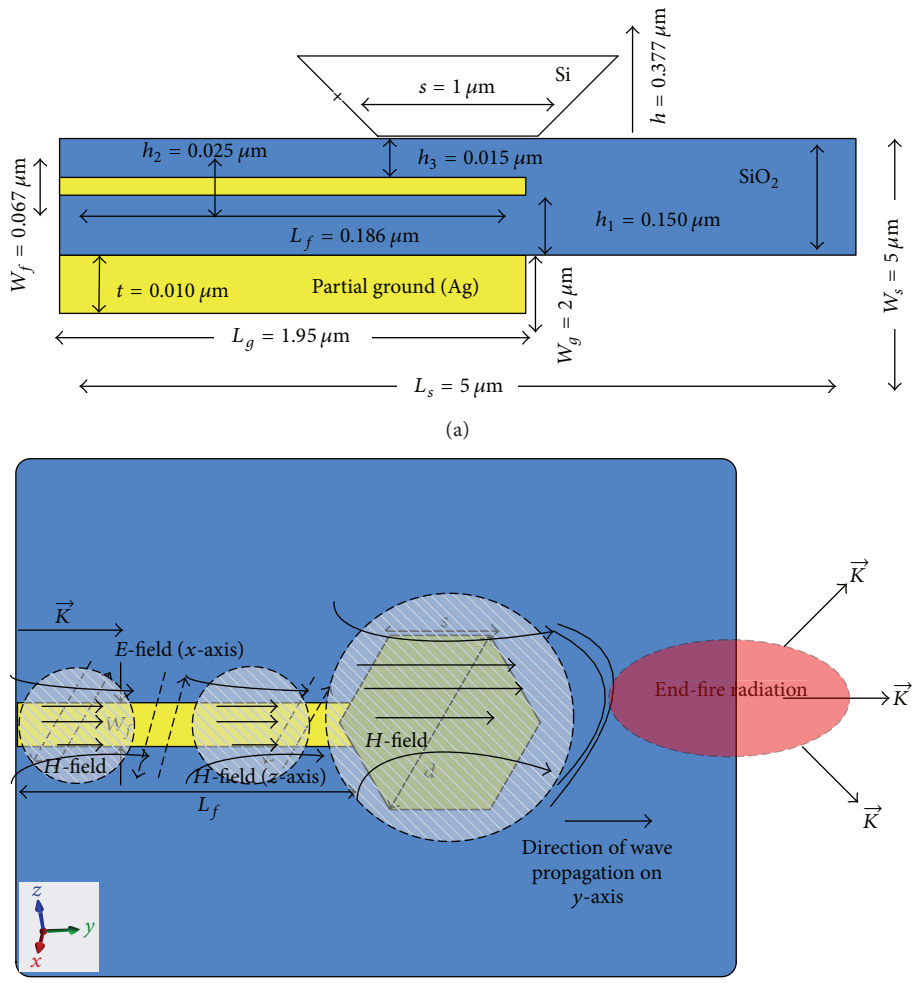

Figure 1: (a) Side view of proposed nantenna with relevant dimensions. (b) Top view of proposed nantenna. Propagation vector K represents the optical power flowing along the y-axis. The E-field and H-field lines are also shown in the x- and z-axis, respectively.

3. Parametric Studies

In this section, we investigate the role of each physical and geometrical parameter in our proposed hexagonal dielectric nantenna structure. The process of optimization was achieved on the various parameters by considering the whole geometric structure as shown in Figure 1(a). In order to study the impact on the antenna performance in terms of bandwidth, the following parameters have been studied and analysed.

3.1. Nanostrip Feed. The silver nanostrip characterized by Drude model was optimized in terms of its length and width. The traditional empirical formulas [3] were used as a starting point for the nanostrip design. The nanostrip acts like a coupling resonator that excites the hexagonal dielectric, placed on an upper SiO_2 substrate with height h_3. Traditionally at RF frequencies the length of the transmission lines is characterized to the wavelengths (λ) of incoming and outgoing radiations. However working at the optical frequencies, the traditional RF wavelength characteristics scenario no longer applies as the incident waves are not perfectly reflected back from the metal's surface. Instead, radiation penetrates into the metal giving rise to the excitation of the free electron gas. Hence at optical frequencies, instead of using the traditional wavelength (λ) we make use of shorter effective wavelength (λ_{eff}) which depends on the material properties [37, 38] given by the following equation for length of a transmission line [39]:

$$\frac{m\lambda_{\text{eff}}}{2} = L(\lambda_0), \tag{3}$$

where (3) shows the relationship between the free space wavelength (λ_0) and the effective wavelength (λ_{eff}) and the order of resonance (m). Here effective wavelength is given by

$$\lambda_{\text{eff}} = \frac{\lambda_0}{n_{\text{eff}}}. \tag{4}$$

Typical values of n_{eff} have been measured to be in the range of 1.5–3 [40]. In our simulation, for the silver nanostrip

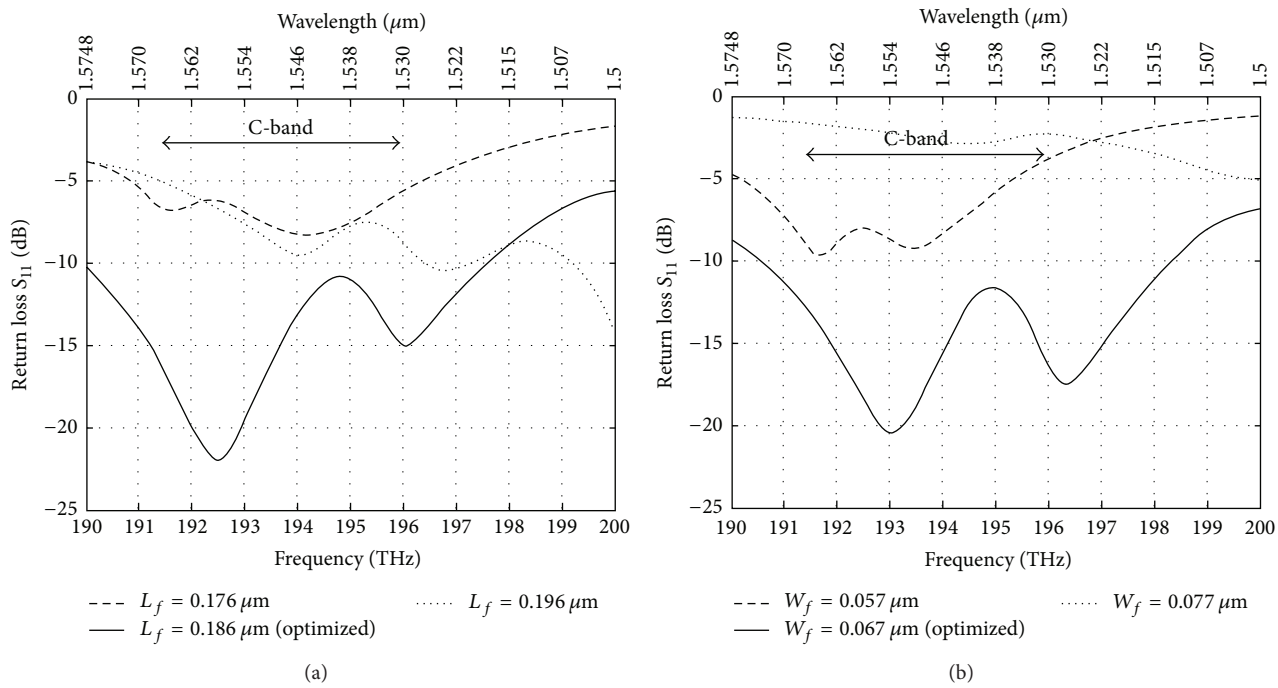

Figure 2: (a) Stub length with optimized values. (b) Width of the nanostrip feed with optimized values.

design, the selected $n_{\text{eff}} = 2.8$ [41] resulting in the minimum resonating length of the nanostrip to be 0.27 μm. The length L_f of the nanostrip stub was optimized from 0.1 μm to 0.27 μm with the best optimized value producing required resonance at 193.5 THz being at $L_f = 0.186\,\mu$m as shown in Figure 2(a).

The effect of the width "W_f" of the nanostrip was also examined by extensive parametric studies. Initial values were taken from the empirical formulas [3] and optimization was done from 0.02 μm to 0.28 μm. Figure 2(b) shows the best optimized value achieved at resonance of −22 dB with $W_f = 0.067\,\mu$m.

3.2. Partial Ground Plane. The effect of the ground plane was studied on the nanoantenna design. Initially a finite ground plane was used to achieve a good radiation pattern with an acceptable bandwidth. The ground plane was then optimized and a partial ground plane was selected with dimensions $L_g \times W_g = 1.95\,\mu\text{m} \times 2\,\mu\text{m}$. Figures 3(a) and 3(b) show the effects of varying the ground plane in terms of its length and width. The optimized results produce a wide impedance bandwidth of 3.7% (190.9 THz–198.1 THz) at a center frequency of 193.5 THz, covering all of the standard optical transmission widow (C-band).

3.3. Height of Hexagonal DR. The wide impedance bandwidth achieved is also affected by the height of the hexagonal DR. The height h of the DR was optimized within the range ($\lambda_g/4 < h < \lambda_g/2$) [3]. Figure 4 shows the best optimized value of $h = 0.37\,\mu$m having a resonance at −23 dB.

4. Results and Discussions

4.1. Comparison with Reference RF Antenna. Initially the reference antenna [25] available at the lower radio frequency spectrum is simulated and its results are noted. Next the proposed nantennas results, achieved as per optimization in the previous section, are compared to the reference antenna. Observations are made in terms of plane wave propagation in the transmission lines to the radiating structures of the two antennas with results shown in Figures 5(a) and 5(b), respectively. From Figure 5(a) it can be observed that the E-field propagation or the power propagation in the transmission line is following the fringing effects in order to radiate the hexagonal structure operating in the microwave domain, whereas the proposed nantenna structure depicted in Figure 5(b) shows that the E-field propagation in the nanotransmission line follows a travelling wave effect. It is also observed that the hexagonal DR elements for both the cases exhibit different properties. At the microwave domain the hexagonal DR as shown in Figure 5(a) works as a resonator while the DR at the nanoscale structure shown in Figure 5(b) exhibits loading properties which benefits the nantenna to operate as a lens and thus achieve more directivity.

4.2. Return Loss S_{11} and Directivity. Figure 6 shows the return loss curve and directivity of the simulated nantenna with respective wavelength and directivity axis. After extensive optimization, the nantenna achieves an impedance bandwidth of 3.7% (190.9 THz–198.1 THz) with a directivity of 8.6 dBi, making it useful for nanoscale fabrication due to its robustness against fabrication tolerances.

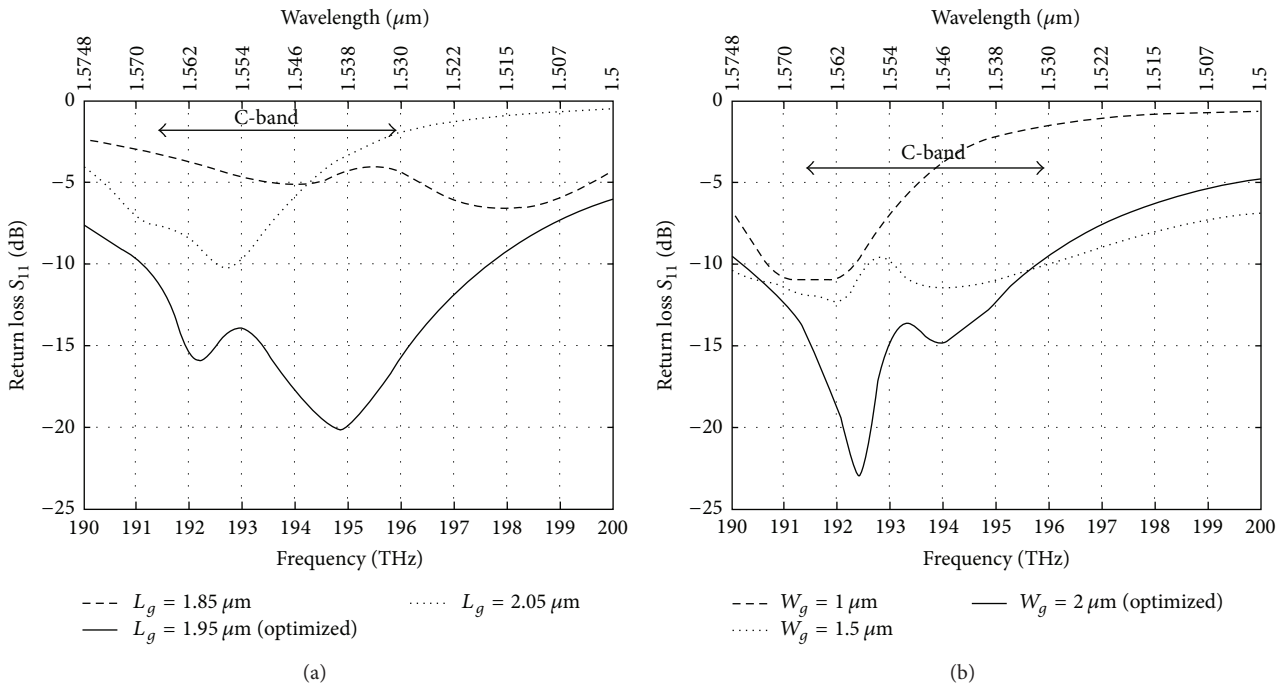

Figure 3: (a) Length of partial ground plane with optimized values. (b) Width of partial ground plane with optimized values.

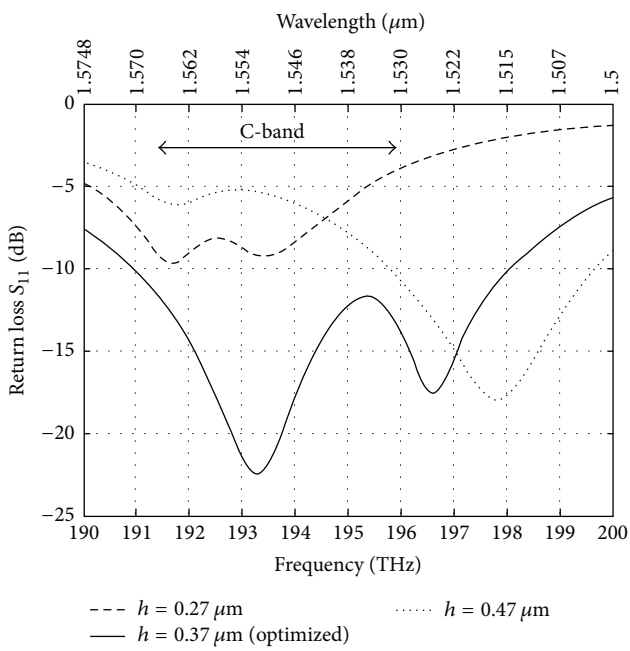

Figure 4: Optimization of height of hexagonal DR.

4.3. Modes of HDLN. Typically, the modes of hexagonal DR [30] are derived from the cylindrical dielectric resonator, which has three distinct types: TE (TE to z), TM (TM to z), and hybrid modes. The TE and TM modes are asymmetrical and have no azimuthal variation. On the other hand, fields produced by hybrid modes are azimuthally dependent. Hybrid mode is further divided into two subgroups of HE and EH [27]. The modes generated by the hexagonal dielectric nantenna are represented in terms of magnitude of electric field distribution on its surface as shown in Figure 7, at the center frequency of 193.5 THz. The mode analysis was done via EM simulator CST MWS.

From the infinite modes available [22], in our simulation as shown in Figure 7, we observed the nanohexagonal dielectric antenna producing $HE_{20\delta}$ mode within the achieved wide impedance band. The subscript in the modes represents the

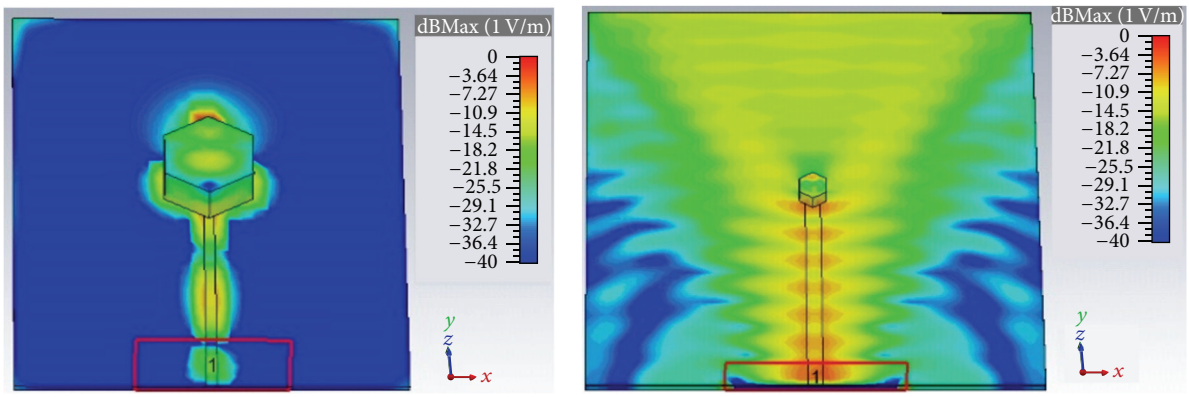

(a) (b)

Figure 5: (a) E-field propagation having fringing effects in the transmission line of a hexagon dielectric resonator at microwave frequencies [25]. (b) E-field propagation having travelling wave effects in the nanostrip transmission line of the proposed nantenna.

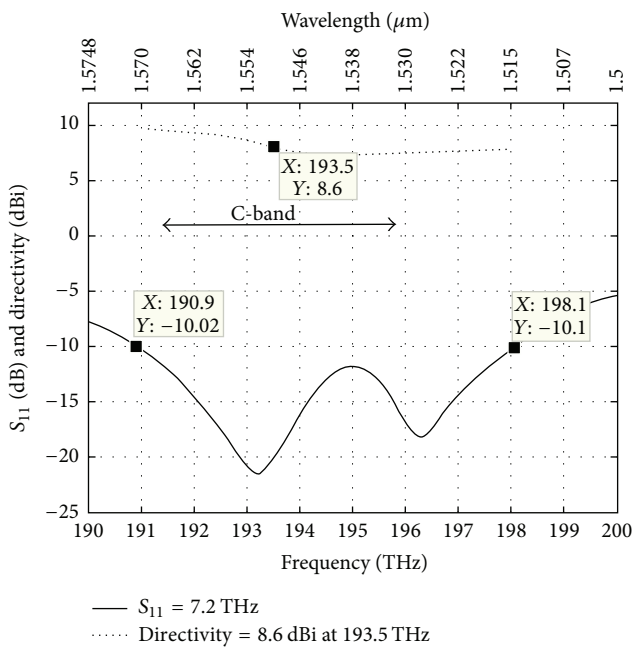

Figure 6: Return loss S_{11} (solid line) and directivity (dotted line) of proposed nantenna.

variation of fields along azimuthal, radial, and z-direction of the cylindrical axis. It is observed from the figure that the magnitude of electric field variation is produced on the azimuthal direction with no variation in the radial direction thus giving a mode excited at $HE_{20\delta}$. Also the intensity is highest at the azimuthal plane resulting in a radiation pattern towards the end-fire direction.

4.4. 3D Radiation Patterns. The 3D radiation patterns of the nanoantenna at 191 THz, 193.5 THz, and 198 THz are shown in Figures 8(a)–8(c). The directivity of the antenna at the center frequency is 8.6 dBi. Examining the 3D radiation patterns in Figure 8 provides the proof of the HDLN radiating in end-fire pattern.

5. Conclusion

In this paper, we proposed and simulated a hexagonal dielectric loaded nantenna for communication among nanodevices in nanonetworks. The nanoantenna is composed of "Ag-SiO_2-Ag" structure with a nanosilver transmission line that excites a hexagonal dielectric made of "Si" material. The antenna exhibits an impedance bandwidth of 3.7% (190.9 THz–198.1 THz) with a directive radiation pattern of 8.6 dBi. Keeping in mind the state-of-the-art nantenna designs and limited availability of nanofabrication equipment and facilities worldwide, we believe that our proposed theoretical HDLN design will prove itself to be a promising communication device for applications based on nanotechnology.

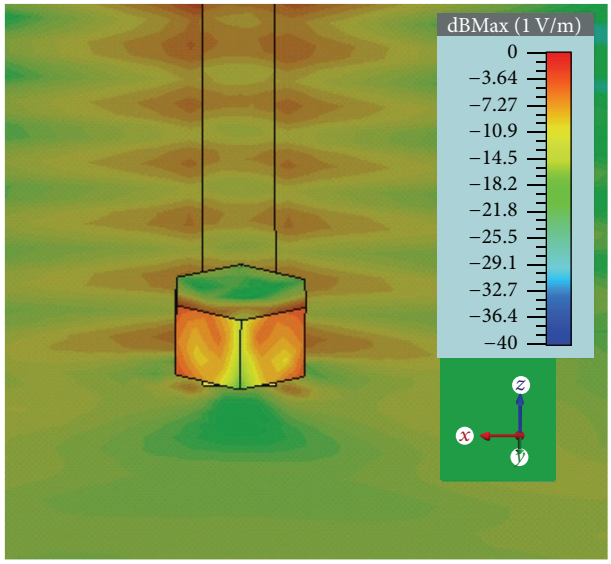

Figure 7: Magnitude of E-field distribution at 193.5 THz with $HE_{20\delta}$ mode.

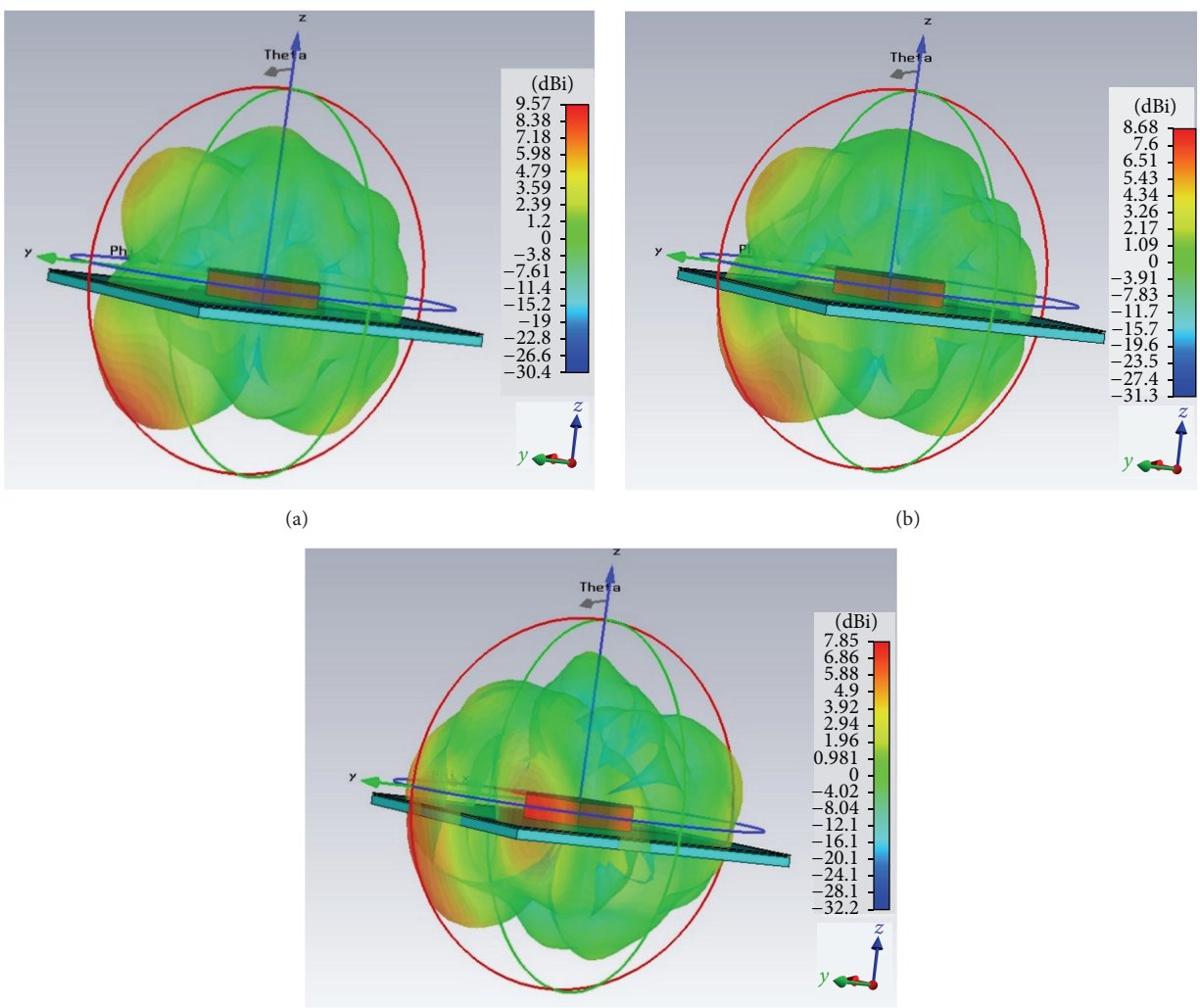

Figure 8: (a) 3D radiation pattern at 191 THz. (b) 3D radiation pattern at 193.5 THz. (c) 3D radiation pattern at 198 THz.

Competing Interests

The authors declare that they have no competing interests.

Acknowledgments

This research is supported by King Abdul Aziz City for Science and Technology (KACST) Technology Innovation Center in RF and Photonics for the e-Society (RFTONICS) hosted at King Saud University.

References

[1] P. Bharadwaj, B. Deutsch, and L. Novotny, "Optical antennas," *Advances in Optics and Photonics*, vol. 1, no. 3, pp. 438–483, 2009.

[2] L. Novotny and N. van Hulst, "Antennas for light," *Nature Photonics*, vol. 5, no. 2, pp. 83–90, 2011.

[3] C. A. Balanis, *Antenna Theory Analysis and Design*, John Wiley & Sons, New York, NY, USA, 2005.

[4] J. Yang, X. Wu, and J. Wu, "Optimal scheduling of collaborative sensing in energy harvesting sensor networks," *IEEE Journal on Selected Areas in Communications*, vol. 33, no. 3, pp. 512–523, 2015.

[5] J. M. Jornet and I. F. Akyildiz, "Graphene-based plasmonic nano-antenna for terahertz band communication in nanonetworks," *IEEE Journal on Selected Areas in Communications*, vol. 31, no. 12, pp. 685–694, 2013.

[6] S. Ulukus, A. Yener, E. Erkip et al., "Energy harvesting wireless communications: a review of recent advances," *IEEE Journal on Selected Areas in Communications*, vol. 33, no. 3, pp. 360–381, 2015.

[7] X. Ren, W. E. I. Sha, and W. C. H. Choy, "Tuning optical responses of metallic dipole nanoantenna using graphene," *Optics Express*, vol. 21, no. 26, pp. 31824–31829, 2013.

[8] F. P. G. de Arquer, V. Volski, N. Verellen, G. A. E. Vandenbosch, and V. V. Moshchalkov, "Engineering the input impedance of optical nano dipole antennas: materials, geometry and excitation effect," *IEEE Transactions on Antennas and Propagation*, vol. 59, no. 9, pp. 3144–3153, 2011.

[9] Y. Yifat, M. Eitan, Z. Iluz, Y. Hanein, A. Boag, and J. Scheuer, "Highly efficient and broadband wide-angle holography using patch-dipole nanoantenna reflectarrays," *Nano Letters*, vol. 14, no. 5, pp. 2485–2490, 2014.

[10] N. Pfullmann, C. Waltermann, M. Noack et al., "Bow-tie nanoantenna assisted generation of extreme ultraviolet radiation," *New Journal of Physics*, vol. 15, Article ID 093027, 2013.

[11] I. S. Maksymov, I. Staude, A. E. Miroshnichenko, and Y. S. Kivshar, "Optical Yagi-Uda nanoantennas," *Journal of Nanophotonics*, vol. 1, no. 1, pp. 1–17, 2012.

[12] B. Lahiri, S. G. McMeekin, R. M. De La Rue, and N. P. Johnson, "Resonance hybridization in nanoantenna arrays based on asymmetric split-ring resonators," *Applied Physics Letters*, vol. 98, no. 15, Article ID 153116, 2011.

[13] E. A. Soliman, "Circularly polarized nanoring antenna for uniform overheating applications," *Microwave and Optical Technology Letters*, vol. 54, no. 9, pp. 2209–2214, 2012.

[14] D. Sikdar, W. Cheng, and M. Premaratne, "Optically resonant magneto-electric cubic nanoantennas for ultra-directional light scattering," *Journal of Applied Physics*, vol. 117, no. 8, Article ID 083101, 2015.

[15] E. Rusak, I. Staude, M. Decker et al., "Hybrid nanoantennas for directional emission enhancement," *Applied Physics Letters*, vol. 105, no. 22, Article ID 221109, 2014.

[16] S.-W. Qu and Z.-P. Nie, "Plasmonic nanopatch array for optical integrated circuit applications," *Scientific Reports*, vol. 3, article 3172, 2013.

[17] F. J. Rodríguez-Fortuño, D. Puerto, A. Griol, L. Bellieres, J. Martí, and A. Martínez, "Sorting linearly polarized photons with a single scatterer," *Optics Letters*, vol. 39, no. 6, pp. 1394–1397, 2014.

[18] R. D. Richtinyer, "Dielectric resonators," *Journal of Applied Phyics*, vol. 10, no. 6, pp. 391–398, 1939.

[19] S. A. Long, M. W. McAllister, and L. C. Shen, "The resonant cylindrical dielectric cavity antenna," *IEEE Transactions on Antennas and Propagation*, vol. 31, no. 3, pp. 406–412, 1983.

[20] A. Petosa, A. Ittipiboon, Y. M. M. Antar, D. Roscoe, and M. Cuhaci, "Recent advances in dielectric-resonator antenna technology," *IEEE Antennas and Propagation Magazine*, vol. 40, no. 3, pp. 35–47, 1998.

[21] K. M. Luk and K. W. Leung, *Dielectric Resonator Antennas*, Research Studies Press, Hertfordshire, UK, 2002.

[22] R. K. Mongia and P. Bhartia, "Dielectric resonator antennas—a review and general design relations for resonant frequency and bandwidth," *International Journal of Microwave and Millimeter-Wave Computer-Aided Engineering*, vol. 4, no. 3, pp. 230–247, 1994.

[23] H. Zhou, Z. Li, L. Shang, A. Mickelson, and D. S. Filipovic, "On-chip wireless optical broadcast interconnection network," *Journal of Lightwave Technology*, vol. 28, no. 24, pp. 3569–3577, 2010.

[24] H. Zhou, X. Chen, D. S. Espinoza, A. Mickelson, and D. S. Filipovic, "Nanoscale optical dielectric rod antenna for on-chip interconnecting networks," *IEEE Transactions on Microwave Theory and Techniques*, vol. 59, no. 10, pp. 2624–2632, 2011.

[25] V. Hamsakutty, A. V. P. Kumar, J. Yohannan, and K. T. Mathew, "Hexagonal dielectric resonator antenna for 2.4 GHz WLAN applications," *Microwave and Optical Technology Letters*, vol. 49, no. 1, pp. 162–164, 2007.

[26] M. W. McAllister, S. A. Long, and G. L. Conway, "Rectangular dielectric resonator antenna," *Electronics Letters*, vol. 19, no. 6, pp. 218–219, 1983.

[27] R. K. Mongia, A. Ittipiboon, Y. M. M. Antar, P. Bhartia, and M. Cuhaci, "Half-split cylindrical dielectric resonator antenna using slot-coupling," *IEEE Microwave and Guided Wave Letters*, vol. 3, no. 2, pp. 38–39, 1993.

[28] A. A. Kishk, G. Zhou, and A. W. Glisson, "Analysis of dielectric-resonator antennas with emphasis on hemispherical structures," *IEEE Antennas and Propagation Magazine*, vol. 36, no. 2, pp. 20–31, 1994.

[29] H. Y. Lo, K. W. Leung, K. M. Luk, and E. K. N. Yung, "Low profile equilateral-triangular dielectric resonator antenna of very high permittivity," *Electronics Letters*, vol. 35, no. 25, pp. 2164–2166, 1999.

[30] V. Hamsakutty and K. T. Mathew, *Hexagonal dielectric resonator antenna—a novel DR antenna for wireless communication [Ph.D. thesis]*, Department of Electronics, Cochin University of Science and Technology, 2007.

[31] P. B. Johnson and R. W. Christy, "Optical constants of the noble metals," *Physical Review B*, vol. 6, no. 12, pp. 4370–4379, 1972.

[32] J. Lloyd-Hughes and T.-I. Jeon, "A review of the terahertz conductivity of bulk and nano-materials," *Journal of Infrared, Millimeter, and Terahertz Waves*, vol. 33, no. 9, pp. 871–925, 2012.

[33] *Computer Simulation Technology, Microwave Studio*, CST, Berlin, Germany, 2012.

[34] H. T. Hattori, Z. Li, D. Liu, I. D. Rukhlenko, and M. Premaratne, "Coupling of light from microdisk lasers into plasmonic nanoantennas," *Optics Express*, vol. 17, no. 23, pp. 20878–20884, 2009.

[35] Z. Li, H. T. Hattori, L. Fu, H. H. Tan, and C. Jagadish, "Merging photonic wire lasers and nanoantennas," *Journal of Lightwave Technology*, vol. 29, no. 18, Article ID 5892863, pp. 2690–2697, 2011.

[36] H. T. Hattori, Z. Li, and D. Liu, "Driving plasmonic nanoantennas with triangular lasers and slot waveguides," *Applied Optics*, vol. 50, no. 16, pp. 2391–2400, 2011.

[37] C. Fumeaux, M. A. Gritz, I. Codreanu, W. L. Schaich, F. J. González, and G. D. Boreman, "Measurement of the resonant lengths of infrared dipole antennas," *Infrared Physics and Technology*, vol. 41, no. 5, pp. 271–281, 2000.

[38] F. Neubrech, T. Kolb, R. Lovrincic et al., "Resonances of individual metal nanowires in the infrared," *Applied Physics Letters*, vol. 89, no. 25, Article ID 253104, 2006.

[39] R. L. Olmon and M. B. Raschke, "Antenna-load interactions at optical frequencies: impedance matching to quantum systems," *Nanotechnology*, vol. 23, no. 44, Article ID 444001, 2012.

[40] F. Neubrech, D. Weber, R. Lovrincic et al., "Resonances of individual lithographic gold nanowires in the infrared," *Applied Physics Letters*, vol. 93, no. 16, Article ID 163105, 2008.

[41] L. Yousefi and A. C. Foster, "Waveguide-fed optical hybrid plasmonic patch nano-antenna," *Optics Express*, vol. 20, no. 16, pp. 18326–18335, 2012.